Membrane potential is important for bacterial cell division

Henrik Strahl and Leendert W. Hamoen[1]

Centre for Bacterial Cell Biology, Institute for Cell and Molecular Biosciences, Newcastle University, Newcastle NE2 4AX, United Kingdom

Edited by Piet A. de Boer, Case School of Medicine, Cleveland, OH, and accepted by the Editorial Board May 27, 2010 (received for review April 21, 2010)

Many cell division-related proteins are located at specific positions in the bacterial cell, and this organized distribution of proteins requires energy. Here, we report that the proton motive force, or more specifically the (trans)membrane potential, is directly involved in protein localization. It emerged that the membrane potential modulates the distribution of several conserved cell division proteins such as MinD, FtsA, and the bacterial cytoskeletal protein MreB. We show for MinD that this is based on the membrane potential stimulated binding of its C-terminal amphipathic helix. This function of the membrane potential has implications for how these morphogenetic proteins work and provide an explanation for the effects observed with certain antimicrobial compounds.

cytoskeleton | MreB | MinD | FtsA | antibiotics

The bacterial cell has a well organized cytoplasm, and the correct localization of proteins is essential for their function, particularly for those involved in morphogenetic processes. Maintenance of this order requires energy, and it is not surprising that proteins that form cytoskeletal structures, or the cell division machinery, consume ATP or GTP. However, the cell division apparatus (1), and bacterial cytoskeletal elements such as MreB (2), are essentially membrane anchored structures, and membrane attachment also plays a critical role in chromosome segregation (3) and regulation of cell division by the Min system (4, 5). These structures are therefore in the vicinity of another fundamental energy source; the proton motive force (pmf). Despite this proximity, nothing was known about the potential role of this force in the regulation of complex protein structures. Indications that the pmf might be important emerged when we were studying the cell division regulator MinD in *Bacillus subtilis*. Cytokinesis in most bacteria is initiated by the polymerization of the tubulin homolog FtsZ into a ring-like structure (the Z-ring) onto which the cytokinesis apparatus assembles (1). The Z-ring should only be formed at midcell in between the newly formed daughter chromosomes, and this process is carefully regulated. In rod-shaped bacteria, the Min system prevents polymerization of FtsZ close to cell poles (5), and the *B. subtilis* MinC and MinD proteins accumulate at cell division sites and cell poles (4). However, we had difficulties reproducing this localization pattern, depending on which methods we used to immobilize the bacterial cells. It appeared that the use of polylysine-coated slides results in loss of polar localization of MinD (Fig. S1). This was surprising because polylysine is generally used to immobilize live cells for microscopy. Similar observations were recently reported by other groups (6, 7). In a different context, it was reported that polylysine can interact with cell membranes and affect the pmf (8). Because this would have important implications for our understanding of the Min system, we decided to analyze this further. It appeared that the pmf is crucial for the normal localization of a number of morphogenetic proteins in different bacterial species and that this is not related to ATP levels in the cell.

Results and Discussion

Role of pmf in Protein Localization. To test whether the pmf is important for the cellular localization of MinD, we analyzed the localization of GFP-MinD in *B. subtilis* cells after the addition of the ionophore carbonyl cyanide m-chlorophenylhydrazone (CCCP). CCCP is a specific proton-ionophore that rapidly dissipates the pmf. The effect on GFP-MinD localization was almost immediately apparent, and within 2 min after addition, the time it normally takes to prepare cells for microscopic observations, the fluorescence signal was diffuse and spotty (Fig. 1). This was similar to what we had observed with polylysine-coated slides (Fig. S1). Apparently, the pmf is indeed essential for the proper localization of MinD. To examine whether this phenomenon is more general, we tested the localization of over 20 different proteins that show a clear localization pattern and that are involved in diverse processes, including cell shape regulation (MreB, Mbl, MreBH, MreC, and MreD), cell division (FtsZ, FtsA, ZapA, SepF, and Pbp2B), cell division regulation (MinD, MinC, DivIVA, MinJ, and EzrA), chromosome segregation (Spo0J and Soj), chromosome replication (PolC), signal transduction (KinA, KinB, and ComK), and others (Hbs, ClpP, ClpX, ClpC, SecA, and AtpA). To follow the localization of these proteins we made use of GFP fusions, most of which have been described in previous studies (see *SI Text* for details). Nine proteins (MinC, MinD, Soj, FtsA, MreB, Mbl, MreBH, MreC, and MreD) showed a rapid change in cellular localization after incubation with CCCP (Fig. 1, Fig. S2, and Table 1).

The protein MinC and the DNA replication initiation regulator Soj both require MinD for their normal cellular localization (3, 9), and the observed influence of CCCP on both is likely due to the delocalization of MinD. Delocalization was also observed for the conserved cell division protein FtsA. FtsA interacts directly with FtsZ and stimulates assembly of the Z-ring (1). Although the YFP-FtsA fusion is recruited to the cell division site, the protein does not fully complement the deletion of *ftsA*. Therefore, we tested the influence of CCCP on FtsA localization using immunofluorescence microscopy as well. Also in this case, the septal fluorescent signal disappeared after the addition of CCCP (Fig. S2). The fluorescent bands formed by GFP-FtsZ did not disappear completely, but the fluorescence signal became weaker after incubation with CCCP. A comparable effect was observed with the FtsZ binding proteins ZapA and SepF. A more quantitative analysis showed that the reduction in fluorescence within the first 2 min coincides with the loss of septal FtsA (Fig. S3). The localization of the integral membrane components of the cell division complex (EzrA and Pbp2B) are not affected by CCCP (Fig. S3).

Interestingly, the cytoskeletal proteins MreB, Mbl, and MreBH, also showed a clear sensitivity for CCCP (Fig. 1 and Fig. S2). These actin homologs form spiral structures immediately underneath the cell membrane and, together with the integral membrane proteins MreC and MreD, coordinate cell wall synthesis (10, 11). The he-

Author contributions: H.S. and L.W.H. designed research; H.S. performed research; H.S. and L.W.H. analyzed data; and H.S. and L.W.H. wrote the paper.

The authors declare no conflict of interest.

This article is a PNAS Direct Submission. P.A.d.B. is a guest editor invited by the Editorial Board.

Freely available online through the PNAS open access option.

[1]To whom correspondence should be addressed. E-mail: l.hamoen@newcastle.ac.uk.

This article contains supporting information online at www.pnas.org/lookup/suppl/doi:10.1073/pnas.1005485107/-/DCSupplemental.

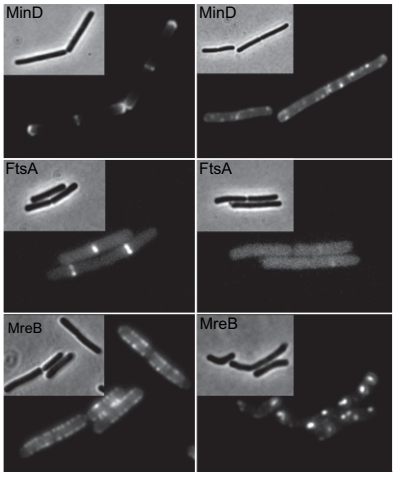

Fig. 1. Pmf-dependent localization of proteins. Cellular localization of GFP-MinD, YFP-FtsA, and GFP-MreB in *B. subtilis* cells in the presence (*Right*) and absence (*Left*) of the proton ionophore CCCP (100 μM). Strains used: *B. subtilis* 1981 (GFP-MinD), *B. subtilis* PG62 (YFP-FtsA), and *B. subtilis* YK405 (GFP-MreB).

lical localization of the latter two proteins also disappeared upon incubation with CCCP (Fig. S2). In summary, the pmf appears to play a distinct role in the localization of important morphogenetic proteins in *B. subtilis*.

Role of pmf Is Independent of Changes in Cellular ATP Levels. All of the proteins that exhibited delocalization upon treatment with CCCP require ATP for their activities. However, the dissipation of the pmf by CCCP can result in a significant decrease of ATP levels in the cell. The F_1F_o ATP-synthase catalyzes the conversion of the pmf into ATP. In the absence of a pmf, the F_1F_o ATP-synthase can also function as an ATP-driven proton pump (12), and this eventually depletes the intracellular ATP-pool. To examine how fast the depletion of ATP takes place, we measured the cellular ATP levels using a luciferase/luciferin assay. As shown in Fig. 2*A*, after 2 min of incubation with CCCP about half the amount of ATP has been consumed, and there seems to be sufficient ATP left for most proteins to function normally. Nevertheless, to rule out that the effect of CCCP is due to a reduction in ATP levels, we repeated the experiments in an F_1F_o ATP-synthase deficient strain. Such strain is able to maintain normal ATP levels by substrate-level phosphorylation when grown in rich medium (13). Indeed, in the F_1F_o ATP-synthase deficient strain, CCCP has almost no effect on ATP levels during the first minutes of incubation (Fig. 2*A*). We transformed the different GFP protein fusions into the F_1F_o ATP-synthase deficient strain and examined the resulting strains by fluorescence microscopy. The CCCP-dependent delocalization of MinD, MinC, Soj, FtsA, FtsZ, MreB, Mbl, and MreBH was identical to the previous experiments (Fig. 2*B* and Fig. S4*A*). Thus, the effect of CCCP is not related to a reduction in ATP levels.

As a final control, we analyzed the localization of a non ATP-binding MinD mutant. The K16A mutation in the conserved ATP-binding Walker-A site abolishes the polar localization of MinD. However, this MinD variant is still able to bind membranes, and a fusion with GFP shows a clear fluorescent membrane signal (9). Addition of CCCP rapidly abolished the membrane signal providing further support for the direct ATP-independent role of the pmf in MinD localization (Fig. 2 *C* and *D*).

Conservation Across Bacterial Species. To test whether the pmf is also important for protein localization in other bacteria, we analyzed the localization of MinD in *Escherichia coli.* The localization of MinD in *E. coli* differs from *B. subtilis* in that the protein displays a rapid pole-to-pole oscillation and a transient membrane binding (14) (Fig. 3*A*). Nevertheless, *E. coli* MinD also exhibited a rapid loss of membrane binding after addition of CCCP, and no pole-to-pole oscillation was observed (Fig. 3*B*). In analogy to the control experiments in *B. subtilis*, the oscillation of MinD in *E. coli* was still sensitive for CCCP in an F_1F_o ATP-synthase deficient strain (Fig. S4*B* and Movie S1). The cell division protein FtsA exhibited a rapid CCCP-dependent delocalization in *E. coli* as well (Fig. 3*C* and Fig. S4*B*). Thus, the importance of the membrane potential for protein localization is not restricted to Gram-positive bacteria.

We also tested the localization of MreB in *E. coli* and *Caulobacter crescentus*. Here, the role of the pmf appeared to be more complex. In *C. crescentus* the MreB localization pattern was rap-

Table 1. Effect of CCCP on protein localization in *B. subtilis*

Protein	Function	Localization	Localization after dissipation of pmf
MreB, Mbl, MreBH, MreC, MreD	Cytoskeleton	Helical clustering	Loss of helicity
MinD, MinC	Septum positioning	Polar/septal	Loss of membrane binding/ polar localization
MinJ, DivIVA	Septum positioning	Polar/septal	No effect
FtsA	Cell division	Septal	Loss of septal localization
FtsZ, ZapA, SepF	Cell division	Septal	Reduction of septal localization
EzrA, Pbp2B	Cell division	Septal	No effect
Spo0J	Chromosome segregation	Clustering/nucleoid	No effect
Soj	Chromosome segregation	Polar/septal	Loss of polar localization
Hbs	Chromatin	Nucleoid	No effect
PolC	DNA replication	Clustering/nucleoid	No effect
ClpP, ClpX, ClpC	Protein degradation	Clustering/polar	No effect
SecA	Protein translocation	Membrane	No effect
AtpA	ATP synthesis	Membrane	No effect
KinA	Sensory kinase/sporulation	Cytoplasmic	No effect
KinB	Sensory kinase/sporulation	Membrane	No effect
ComK	Transcription factor	Nucleoid	No effect
TlpA	Chemoreceptor/chemotaxis	Polar/membrane	No effect

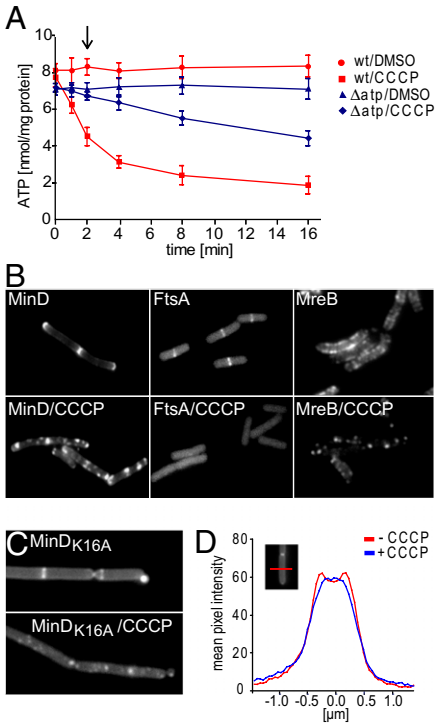

Fig. 2. Pmf-dependent localization of proteins is independent of ATP levels. (*A*) Cellular ATP-levels of wild-type (red) and an F_1F_o ATP synthase-deficient *B. subtilis* strain (blue) upon dissipation of the pmf with CCCP (100 μM in DMSO). As a control the cells were incubated with DMSO (0.1%). (*B*) Effect of CCCP on the localization of GFP-MinD, YFP-FtsA, and GFP-MreB in the F_1F_o ATP synthase-deficient strain background. Images were taken within 2 min (indicated with an arrow in *A*). Strains used: *B. subtilis* HS14 (GFP-MinD), *B. subtilis* HS20 (YFP-FtsA), and *B. subtilis* HS23 (GFP-MreB). (*C*) Cellular localization of the non-ATP-binding GFP-$MinD_{K16A}$ in the presence and absence of CCCP (100 μM). (*D*) The average fluorescence intensity profile of GFP-$MinD_{K16A}$ measured diagonal to the length of the cells (n = 40). Strain used: *B. subtilis* HS15 (GFP-$MinD_{K16A}$).

idly influenced after CCCP addition (Fig. 3*D*), but in *E. coli* CCCP had no effect on the localization of MreB, MreC, or MreD (Fig. S2*B*). Nevertheless, these results suggest that the influence of the pmf on protein localization is widespread among bacteria.

Effect on Protein Localization Is Not Restricted to CCCP. To exclude that the observed changes in cellular localization patterns were caused by an unspecific (pmf unrelated) influence of CCCP, we tested other ionophores that are known to dissipate the pmf. The activity of the channel forming polycyclic peptide antibiotic nisin (15) resulted in the same delocalization of MinD, FtsA, and MreB as seen with CCCP (Fig. S5*A*). The bacteriocin colicin N is a channel forming toxin that is known to dissipate the membrane potential in *E. coli* (16), and addition of colicin N completely abolished MinD oscillation and septal localization of FtsA (Fig. S5*B* and Movie S1). The ionophore valinomycin also abolished the normal localization of MinD, FtsA, and MreB (see below). Therefore, we can now conclude that observed delocalization effect is indeed related to the dissipation of the pmf.

Membrane Potential Is the Responsible Key Factor. The pmf is composed of the transmembrane chemical proton gradient (ΔpH) and the transmembrane electric potential (ΔΨ). CCCP increases the proton permeability of the membrane thereby dissipating both the ΔpH and ΔΨ. To differentiate which one of these components of the pmf is involved in protein localization, we repeated the experiments using ionophores that specifically modify either the ΔpH

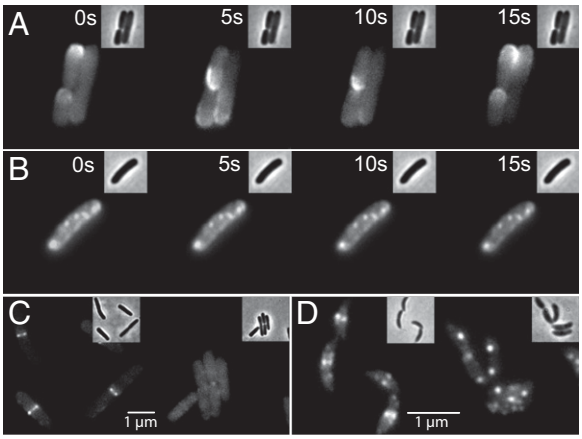

Fig. 3. Pmf-dependent localization of MinD and FtsA in *E. coli* and MreB in *C. crescentus*. (*A*) Pole-to-pole oscillation of *E. coli* GFP-MinD in cells without the proton ionophore CCCP, and (*B*) absence of pole-to-pole oscillation after addition of CCCP (100 μM). Strain used: *E. coli* RC1/pFX9. (*C*) Cellular localization of *E. coli* GFP-FtsA and (*D*) *C. crescentus* GFP-MreB in the presence (*Right*) and absence (*Left*) of CCCP (100 μM). Strains used: *E. coli* MC1000/pHJS101 and *C. crescentus* LS3814.

or the ΔΨ. Nigericin is an antibiotic that facilitates an electroneutral exchange of H^+- and K^+-ions, thereby depleting the ΔpH across the membrane (17). In contrast, the antibiotic valinomycin functions as a K^+-carrier that specifically dissipates the ΔΨ in the presence K^+ ions (18). All tested proteins that featured CCCP-dependent changes in localization pattern were also sensitive to valinomycin, whereas dissipation of the ΔpH by nigericin had no influence (Fig. 4 and Fig. S6*A*). Furthermore, the delocalization caused by valinomycin only took place in the presence of sufficient K^+ in the medium, thereby excluding an unspecific influence of valinomycin (Fig. S6*B*). The activity of both valinomycin and nigericin in *B. subtilis* were confirmed using fluorimetric assays (Fig. S7).

Mechanism of ΔΨ-Dependent Membrane Binding. Such striking effects of the membrane potential on protein localization have not been demonstrated before, and it is rather challenging to suggest mechanisms that could possibly be involved. In *B. subtilis*, MreB forms a complex helical structure together with Mbl, MreBH, MreC, and MreD (10, 11). It is tempting to speculate that the latter two proteins are responsible for the membrane potential sensitivity because both are integral membrane proteins required for the helical localization of MreB and Mbl (19), but why MreC and MreD are sensitive, we do not know. However, it is not a general phenomenon for transmembrane proteins because the localization of AtpA, KinB, MinJ, and TlpA is not affected by CCCP.

In case of MinD and FtsA, the association with the membrane is driven by a membrane binding amphipathic helix at their C-termini (20, 21). Amphipathic helices can bind to membranes

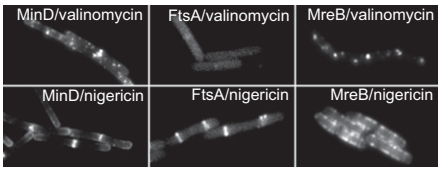

Fig. 4. Pmf-dependent changes in localization are due to changes in membrane potential (ΔΨ). Cellular localization of GFP-MinD, YFP-FtsA and GFP-MreB in *B. subtilis* cells with the ΔΨ dissipated by valinomycin (*Upper*) or the ΔpH dissipated by nigericin (*Lower*). Strains used: *B. subtilis* 1981 (GFP-MinD), *B. subtilis* PG62 (YFP-FtsA), and *B. subtilis* YK405 (GFP-MreB).

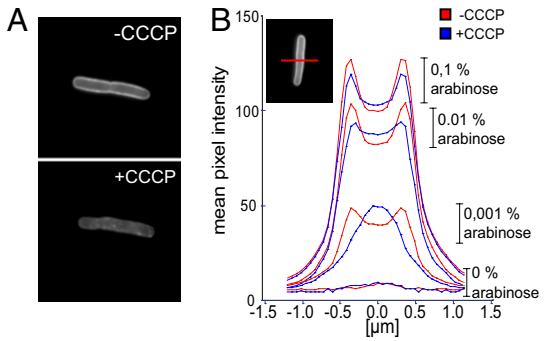

Fig. 5. Membrane potential-dependent localization of the C-terminal amphipathic helix of MinD. (*A*) Localization of a GFP fusion with the C-terminal amphipathic helix of *B. subtilis* MinD expressed in *E. coli* in the presence and absence of CCCP (*Left*). (*B*) Average fluorescence intensity profiles at different induction levels (0.1%, 0.01%, 0.001%, and 0% arabinose) are shown (n = 25). Strain used: *E. coli* PB114/pHJS100.

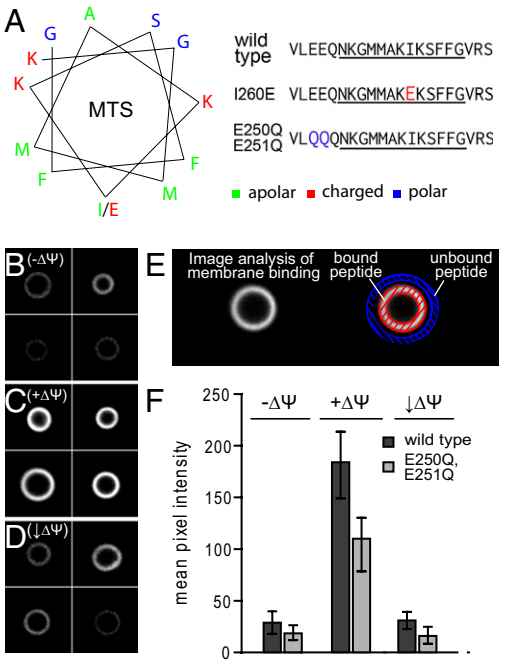

Fig. 6. ΔΨ-stimulated binding of the MinD C-terminal amphipathic helix to liposomes. (*A*) Peptide sequence of the wild-type C-terminal amphipathic helix of MinD and of peptides carrying the I260E and E250Q/E251Q exchanges. The predicted amphipathical regions are underlined and presented as a helical wheel diagram. Binding of a fluorescently labeled synthetic peptide comprising the wild-type C-terminal amphipathic helix of *B. subtilis* MinD to liposomes in the absence (*B*) (−ΔΨ) and presence (*C*) (+ΔΨ) of an artificially induced membrane potential and after dissipation of the membrane potential (*D*) (↓ΔΨ) (see *Materials and Methods* for details). (*E*) Schematic representation of membrane binding measurement by image analysis of the confocal micrographs. (*F*) Mean membrane binding measured for liposomes (n = 50) without membrane potential (−ΔΨ), after induction of the membrane potential (+ΔΨ) and after dissipation of the membrane potential (↓ΔΨ), for wild-type peptide and for a synthetic peptide carrying the E250Q/E251Q exchanges. No binding was detectable for a synthetic peptide carrying the I260E exchange and it is therefore not shown in the diagram.

by burying their apolar side into the lipid bilayer. Lipid binding is further stabilized by charged residues that electrostatically interact with the charged lipid head groups. As a consequence, these membrane targeting motifs allow a reversible and regulated membrane binding that is influenced by both lipid composition and physical properties of the membrane (22, 23). If the membrane binding amphipathic helices are responsible for the ΔΨ-sensitive localization, we might be able to observe this with a GFP fusion to the amphipathic helix alone. Previously, it was shown that a fusion between GFP and the C-terminal amphipathic helix of *E. coli* MinD results in a fluorescent membrane signal (20). In this construct, the amphipathic helix was preceded by the Jun leucine-zipper dimerization domain because it was shown that the ATP dependent dimerization of MinD is important for membrane binding (24). We used this construct and replaced the amphipathic helix of *E. coli* MinD with the amphipathic helix of *B. subtilis* MinD. This fusion protein gave a clear fluorescent membrane signal in *E. coli* cells as well. Addition of CCCP resulted in a rapid reduction of the membrane signal, suggesting that the amphipathic helix is sensitive for the membrane potential (Fig. 5). It should be mentioned that this effect diminished with increasing expression levels of the protein. Several studies have indicated that membrane association of MinD is a cooperative process (25, 26). Because high protein concentrations stimulate cooperative binding, this could explain why the effect of CCCP depends on expression levels.

The complexity of the cytoplasm makes it difficult to exclude other factors that might influence the ΔΨ-dependent interaction of amphipathic helices with the cell membrane. Therefore, we analyzed ΔΨ-dependent lipid binding in vitro using a synthetic peptide comprising the 21 residue–long C-terminal amphipathic helix of MinD attached to a fluorescent 5-FAM group (Fig. 6*A*). When this synthetic peptide was incubated with liposomes, a clear membrane association was observed (Fig. 6 *B* and *F*). Importantly, upon induction of a ΔΨ, the membrane binding increased five- to sixfold (Fig. 6 *C* and *F*). Dissipation of the ΔΨ reduced the membrane signal back to basal levels (Fig. 6 *D* and *F*). As a negative control, we synthesized a peptide in which the hydrophobic isoleucine residue was replaced with a charged glutamate (I260E), thereby disrupting the amphipathic character if this sequence (Fig. 6*A*). Such permutation turned out to be sufficient to abolish membrane binding of MinD in *B. subtilis* cells (Fig. S8). When this mutated synthetic peptide was incubated with liposomes no measurable binding was observed. Applying an artificial membrane potential gave no improvement, thus the amphipathic character of the peptide is essential for both membrane binding and ΔΨ-stimulated association. The amphipathic helix of MinD is preceded by two glutamate residues. To test whether these two negative charges are important for sensing the membrane potential, we synthesized a peptide in which the two glutamates were replaced by two glutamines (E250Q and E251Q). These replacements resulted in a slightly weaker membrane binding but had no effect on the ΔΨ-dependent membrane association of this amphipathic helix (Fig. 6*F*). We have also tested whether these two glutamine substitutions affect GFP-MinD localization in vivo but we found no effect (Fig. S8). The exact mechanism underlying ΔΨ-dependent membrane binding of this amphipathic helix is unclear. Possibly, the membrane potential results in a subtle conformational change of the amphipathic helix that enhances binding. On the other hand, it has been shown that binding of MinD is stimulated when the membrane fluidity is increased (27). Interestingly, membrane fluidity can also be increased by imposing a ΔΨ (28). So it might be that the membrane potential changes the lipid membrane properties, which facilitates the insertion of amphipathic helices. Further studies will be necessary to determine the mechanism of ΔΨ-stimulated membrane binding of amphipathic helices.

Effect of Oxygen Depletion. A major environmental factor that can influence the membrane potential is the availability of utilizable electron acceptor such as oxygen. In soil, the natural habitat of *B. subtilis*, the oxygen levels fluctuate constantly, for instance due to rainfall. To simulate this effect, we depleted *B. subtilis* for oxygen

by flushing cells with argon. In the absence of oxygen, cells became elongated suggesting an effect on cell division. Indeed, microscopic analysis showed that after about 30 min, MinD, FtsA, and MreB were delocalized (Fig. 7 and Fig. S9). After extended oxygen depletion (45–60 min), some cells became wide and bulgy, which is characteristic for MreB depleted cells (10, 11, 19). These effects were reversible and reaeration of the culture for 30 min restored the membrane potential and localization of proteins (Fig. S9). Such morphological changes in *B. subtilis* cells upon oxygen depletion have been documented before (29, 30) and can now be explained by the importance of the membrane potential for protein localization.

Conclusions

Our data reveal a role for the membrane potential in the spatial organization of cytoskeletal and cell division proteins. In case of MinD, we show that the membrane potential stimulates the interaction between the C-terminal amphipathic helix and the lipid bilayer. Because FtsA also binds to the cell membrane by means of a C-terminal amphipathic helix, it is likely that the sensitivity of FtsA for the membrane potential resides on the same mechanism. Membrane targeting amphipathic helices are common. The sensitivity of these membrane anchors for the membrane potential is possibly a more general phenomenon that needs to be taken into consideration. Several *in silico* models for the *E. coli* Min system have been published, and the Min proteins show fascinating dynamic interactions on artificial lipid bilayer supports (31, 32). However, to faithfully reconstruct the Min system, it is now important to include the membrane potential as an additional modulating parameter.

Finally, in their natural environment, microorganisms encounter a large variety of molecules with antibacterial activities. Many of these antibiotics are targeting the cell membrane and dissipate the membrane potential (33). Incubation of *B. subtilis* with the natural antibiotic nisin results in elongated cells and minicells, indicative of a malfunctioning Min system (34). In case of *Spiroplasma*, antibiotics like gramicidin S, mellitin, alamethicin, and valinomycin induce changes in cell morphology (35). It seems now likely that these effects are caused by the delocalization of morphogenetic proteins resulting from dissipation of the membrane potential. This knowledge will be valuable for our understanding of the function of membrane targeting antibiotics and for the development of others.

Materials and Methods

Bacterial Strains, Growth Conditions, and Media. All *B. subtilis* and *E. coli* strains are described in Table S1 and were grown in LB at 30 °C with the following exceptions. *B. subtilis* F_1F_o ATP synthase-deficient strains and cultures depleted for oxygen were grown in LB supplemented with 0.1% glucose. If the influence of valinomycin or nigericin was to be tested, cells were grown in LB supplemented with 50 mM Hepes-HCl pH 7.5, and 300 mM KCl or NaCl. *C. crescentus* was grown as described by Gitai et al. (36). Transformation of *B. subtilis* cells was carried out by the method of Anagnostopoulos and Spizizen (37) as modified by Hamoen et al. (38). DNA manipulation and *E. coli* transformation were performed by standard methods (39). Dissipation of pmf was carried out by the addition of 100 μM CCCP, 375 nM nisin, or 250–1,000 molecules/cell of purified colicin N. The ΔΨ was dissipated specifically by addition 30 μM valinomycin and ΔpH dissipated specifically by addition of 5 μM nigericin. The functionality of CCCP, valinomycin, and nigericin was verified by their growth inhibitory effect. In addition, the dissipation of ΔΨ by valinomycin was analyzed with the potential sensitive fluorescent dye 3,3′-dipropylthiadicarbocyanine iodide $DiSC_3(5)$ and fluorescence microscopy or fluorimetric measurement (Fig. S7*A*, see *SI Text* for details). The activity of nigericin was analyzed fluorometrically with the pH sensitive dye BCECF-AM (Fig. S7*B*, see *SI Text* for details). The depletion of oxygen was carried out by purging midlog phase *B. subtilis* cultures with a constant stream of argon for 30–60 min.

Fluorescence Microscopy. For fluorescence microscopy, cells were grown to midexponential phase at 30 °C and mounted on microscope slides covered with a thin film of 1.2% agarose supplemented with 0.1% DMSO or 100 μM CCCP dissolved in DMSO (0.1% final concentration of DMSO). If valinomycin or nigericin was used, the cells were mounted on 1.2% agarose in 50 mM Hepes-HCl pH 7.5, 300 mM KCl, or NaCl, 0.1% glucose and 0.1% DMSO, 30 μM valinomycin or 5 μM nigericin dissolved in DMSO. If CCCP, valinomycin, or nigericin was used, the cells were supplemented with the corresponding amount of CCCP, valinomycin, nigericin or DMSO before mounting on microscope slides. Immobilization of cells using poly-l-lysine was carried out using 0.1% poly-l-lysine solution (Sigma-Aldrich) following manufacturers' instructions. The imaging was carried out within 2 min after addition of ionophores unless stated differently. The absence of lysis after addition of ionophores was verified by microscopy; no lysis was detectable over a 15-min time period. For the visualization of ΔΨ using potential sensitive fluorescent dye $DiSC_3(5)$, cells were incubated 5 min with 2 μM $DiSC_3(5)$ followed by addition of ionophores. Fluorescence microscopy was carried out using Zeiss Axiovert 200M, Nikon Eclipse Ti-U spinning disk confocal microscope, or Applied Precision DeltaVision RT automated microscope. The images were acquired with Metamorph 6 (Molecular Devices, Inc), FRAP-AI 7 (MAG Biosystems), and softWoRx Suite (Applied Precision) software, and analyzed using ImageJ v.1.38 (National Institutes of Health). If required, optical sectioning and deconvolution was carried out using Huygens Essentials v.3.3 (Scientific Volume Imaging).

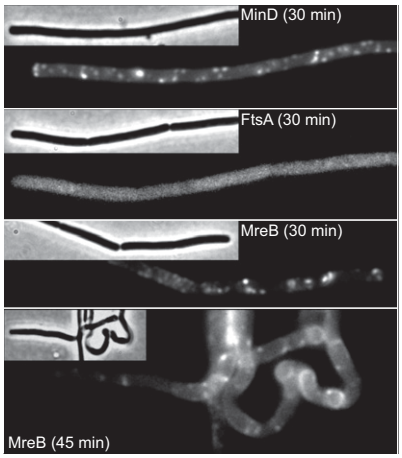

Fig. 7. Effect of oxygen depletion on the localization of MinD, FtsA, and MreB. Localization of GFP-MinD, YFP-FtsA and GFP-MreB in *B. subtilis* cells after 30 min depletion of oxygen. Longer oxygen depletion (45–60 min) resulted in a subpopulation of wide and bulgy cells. Strains used: *B. subtilis* 1981 (GFP-MinD), *B. subtilis* PG62 (YFP-FtsA), and *B. subtilis* YK405 (GFP-MreB).

Lipid Binding Experiments. All lipid binding experiments were carried out with large unilamellar vesicles prepared from *E. coli* polar lipid extract (Avanti) essentially as described in (40). Dry lipid extract was solubilized in chloroform followed by evaporation of chloroform under argon stream. Dry lipids were resolubilized in 50 mM Tris/HCl pH 7.5, 2 mM β-mercaptoethanol, 1.5% octylglycoside (20 mg/mL lipids) under argon stream and dialyzed against 50 mM Tris/HCl pH 7.5, 2 mM β-mercaptoethanol. For binding assays, preformed liposomes (10 mg/mL) were loaded and sized by extrusion through a 0.4-μm membrane in the presence of 25 mM Tris/HCl pH 7.5, 100 mM sucrose, and 150 mM Na_2SO_4 or K_2SO_4. An inside-positive transmembrane potential was induced by 1:50 dilution of Na_2SO_4-loaded liposomes in 25 mM Tris/HCl pH 7.5, 100 mM glucose, 150 mM K_2SO_4, 0.2 μM valinomycin, 1 mg/mL BSA, and 10 μg/mL 5-carboxyfluorescein (5-FAM)-labeled synthetic peptides (Biomatik) corresponding to the membrane targeting amphipathic helix of *B. subtilis* MinD (Table S2). The final molar ratios of lipid:BSA:MTS in the binding experiments were 50:4:1. Liposomes loaded with K_2SO_4 were diluted in the same buffer to analyze the binding of the synthetic peptide to liposomes without transmembrane potential. In addition, the release of bound peptide from liposomes was analyzed by dissipation of the valinomycin-induced transmembrane potential by a subsequent addition of 1 μM nigericin. The microscopy of the liposomes was carried out using Nikon Eclipse Ti-U spinning disk confocal microscope using 491-nm excitation laser (100 ms) and Yokogawa eGFP-emission filter. Image analysis was carried out using ImageJ by measuring the fluorescence mean pixel intensity of 50 individual liposomes. The background of unbound peptide was subtracted by measuring the mean

pixel intensity of a corresponding area surrounding each liposome. The lipid-binding of 5-FAM-MTS peptide was verified by incubating the liposomes with identical amount of free 5-FAM. The ability of the prepared liposomes to generate and maintain transmembrane potential was verified by diluting the K_2SO_4-loaded liposomes 1:100 in corresponding buffer with K_2SO_4 replaced by Na_2SO_4. The induction of inside-negative transmembrane potential after addition of 0.2 μM valinomycin, and the dissipation of the potential by 1 μM nigericin, was measured following the fluorescence of a potential sensitive dye $DiSC_3(5)$ used at concentration of 0.25 μM (Fig. S7*C*).

ACKNOWLEDGMENTS. We thank Christopher Johnson (Newcastle University) for the generous gift of purified colicin N, and Heath Murray (Newcastle University), Sven Halbedel (Robert Koch Institute, Wernigerode, Germany), and Jan-Willem Veening (University of Groningen, Groningen, The Netherlands) for strains. We thank Jeremy Lakey (Newcastle University) and Marc Bramkamp (University of Cologne, Cologne, Germany) for critical reading of the manuscript. Funding for this research was provided by a Wellcome Trust Research Career Development Fellowship for L.W.H. and a Biotechnology and Biological Sciences Research Council Grant in the framework of the Systems Biology of Microorganisms program for H.S.

1. Adams DW, Errington J (2009) Bacterial cell division: Assembly, maintenance and disassembly of the Z ring. *Nat Rev Microbiol* 7:642–653.
2. Grauman PL (2008) Cytoskeletal elements in bacteria. *Annu Rev Microbiol* 61:589–618.
3. Murray H, Errington J (2008) Dynamic control of the DNA replication initiation protein DnaA by Soj/ParA. *Cell* 135:74–84.
4. Marston AL, Thomaides HB, Edwards DH, Sharpe ME, Errington J (1998) Polar localization of the MinD protein of *Bacillus subtilis* and its role in selection of the mid-cell division site. *Genes Dev* 12:3419–3430.
5. Lutkenhaus J (2007) Assembly dynamics of the bacterial MinCDE system and spatial regulation of the Z ring. *Annu Rev Biochem* 76:539–562.
6. Gregory JA, Becker EC, Pogliano K (2008) *Bacillus subtilis* MinC destabilizes FtsZ-rings at new cell poles and contributes to the timing of cell division. *Genes Dev* 22:3475–3488.
7. Colville K, Tompkins N, Rutenberg AD, Jericho MH (2010) Effects of poly(L-lysine) substrates on attached *Escherichia coli* bacteria. *Langmuir* 26:2639–2644.
8. Katsu T, Tsuchiya T, Fujita Y (1984) Dissipation of membrane potential of *Escherichia coli* cells induced by macromolecular polylysine. *Biochem Biophys Res Commun* 122: 401–406.
9. Karoui ME, Errington J (2001) Isolation and characterization of topological specificity mutants of minD in *Bacillus subtilis*. *Mol Microbiol* 42:1211–1221.
10. Leaver M, Errington J (2005) Roles for MreC and MreD proteins in helical growth of the cylindrical cell wall in *Bacillus subtilis*. *Mol Microbiol* 57:1196–1209.
11. Kawai Y, Daniel RA, Errington J (2009) Regulation of cell wall morphogenesis in *Bacillus subtilis* by recruitment of PBP1 to the MreB helix. *Mol Microbiol* 71:1131–1144.
12. Hicks DB, Cohen DM, Krulwich TA (1994) Reconstitution of energy-linked activities of the solubilized F1F0 ATP synthase from *Bacillus subtilis*. *J Bacteriol* 176:4192–4195.
13. Santana M, et al. (1994) *Bacillus subtilis* F0F1 ATPase: DNA sequence of the atp operon and characterization of atp mutants. *J Bacteriol* 176:6802–6811.
14. Hu Z, Lutkenhaus J (1999) Topological regulation of cell division in *Escherichia coli* involves rapid pole to pole oscillation of the division inhibitor MinC under the control of MinD and MinE. *Mol Microbiol* 34:82–90.
15. Hasper HE, et al. (2006) An alternative bactericidal mechanism of action for lantibiotic peptides that target lipid II. *Science* 313:1636–1637.
16. Schein SJ, Kagan BL, Finkelstein A (1978) Colicin K acts by forming voltage-dependent channels in phospholipid bilayer membranes. *Nature* 276:159–163.
17. Harold FM (1970) Antimicrobial agents and membrane function. *Adv Microb Physiol* 4:45–104.
18. Shapiro HM (1994) Cell membrane potential analysis. *Methods Cell Biol* 41:121–133.
19. Defeu Soufo HJ, Graumann PL (2005) *Bacillus subtilis* actin-like protein MreB influences the positioning of the replication machinery and requires membrane proteins MreC/D and other actin-like proteins for proper localization. *BMC Cell Biol* 6:10.
20. Szeto TH, Rowland SL, Habrukowich CL, King GF (2003) The MinD membrane targeting sequence is a transplantable lipid-binding helix. *J Biol Chem* 278:40050–40056.
21. Pichoff S, Lutkenhaus J (2005) Tethering the Z ring to the membrane through a conserved membrane targeting sequence in FtsA. *Mol Microbiol* 55:1722–1734.
22. Johnson JE, Cornell RB (1999) Amphitropic proteins: Regulation by reversible membrane interactions (review). *Mol Membr Biol* 16:217–235.
23. Cornell RB, Taneva SG (2006) Amphipathic helices as mediators of the membrane interaction of amphitropic proteins, and as modulators of bilayer physical properties. *Curr Protein Pept Sci* 7:539–552.
24. Hu Z, Lutkenhaus J (2003) A conserved sequence at the C-terminus of MinD is required for binding to the membrane and targeting MinC to the septum. *Mol Microbiol* 47:345–355.
25. Lackner LL, Raskin DM, de Boer PA (2003) ATP-dependent interactions between Escherichia coli Min proteins and the phospholipid membrane in vitro. *J Bacteriol* 185: 735–749.
26. Mileykovskaya E, et al. (2003) Effects of phospholipid composition on MinD-membrane interactions *in vitro* and *in vivo*. *J Biol Chem* 278:22193–22198.
27. Mazor S, et al. (2008) Mutual effects of MinD-membrane interaction: II. Domain structure of the membrane enhances MinD binding. *Biochim Biophys Acta* 1778: 2505–2511.
28. Schäffer E, Thiele U (2004) Dynamic domain formation in membranes: Thickness-modulation-induced phase separation. *Eur Phys J E Soft Matter* 14:169–175.
29. Hoffmann T, Troup B, Szabo A, Hungerer C, Jahn D (1995) The anaerobic life of *Bacillus subtilis*: Cloning of the genes encoding the respiratory nitrate reductase system. *FEMS Microbiol Lett* 131:219–225.
30. Shingaki R, et al. (2003) Induction of L-form-like cell shape change of *Bacillus subtilis* under microculture conditions. *Microbiology* 149:2501–2511.
31. Kruse K, Howard M, Margolin W (2007) An experimentalist's guide to computational modelling of the Min system. *Mol Microbiol* 63:1279–1284.
32. Loose M, Fischer-Friedrich E, Ries J, Kruse K, Schwille P (2008) Spatial regulators for bacterial cell division self-organize into surface waves *in vitro*. *Science* 320:789–792.
33. Lohner K (2009) New strategies for novel antibiotics: Peptides targeting bacterial cell membranes. *Gen Physiol Biophys* 28:105–116.
34. Hyde AJ, Parisot J, McNichol A, Bonev BB (2006) Nisin-induced changes in *Bacillus* morphology suggest a paradigm of antibiotic action. *Proc Natl Acad Sci USA* 103: 19896–19901.
35. Béven L, Wróblewski H (1997) Effect of natural amphipathic peptides on viability, membrane potential, cell shape and motility of mollicutes. *Res Microbiol* 148:163–175.
36. Gitai Z, Dye N, Shapiro L (2004) An actin-like gene can determine cell polarity in bacteria. *Proc Natl Acad Sci USA* 101:8643–8648.
37. Anagnostopoulos C, Spizizen J (1961) Requirements for Transformation in *Bacillus subtilis*. *J Bacteriol* 81:741–746.
38. Hamoen LW, Smits WK, de Jong A, Holsappel S, Kuipers OP (2002) Improving the predictive value of the competence transcription factor (ComK) binding site in *Bacillus subtilis* using a genomic approach. *Nucleic Acids Res* 30:5517–5528.
39. Sambrook J, Fritsch EF, Maniatis T (1989) *Molecular Cloning: A Laboratory Manual* (Cold Spring Harbor Laboratory Press, Cold Spring Harbor, NY).
40. Heitkamp T, et al. (2008) K^+-translocating KdpFABC P-type ATPase from *Escherichia coli* acts as a functional and structural dimer. *Biochemistry* 47:3564–3575.